Werk

Jahr: 1976
Kollektion: fid.geo
Signatur: 8 Z NAT 2148:42
Digitalisiert: Niedersächsische Staats- und Universitätsbibliothek Göttingen
Werk Id: PPN1015067948_0042
PURL: http://resolver.sub.uni-goettingen.de/purl?PPN1015067948_0042

LOG Id: LOG_0094
LOG Titel: [Plasma disturbances caused by Helios in the solar wind] Seiten 581-582 fehlen
LOG Typ: article

Übergeordnetes Werk

Werk Id: PPN1015067948
PURL: http://resolver.sub.uni-goettingen.de/purl?PPN1015067948
OPAC: http://opac.sub.uni-goettingen.de/DB=1/PPN?PPN=1015067948

Contact

Niedersächsische Staats- und Universitätsbibliothek Göttingen
Georg-August-Universität Göttingen
Platz der Göttinger Sieben 1
37073 Göttingen
Germany
Email: gdz@sub.uni-goettingen.de

2. Calculation of the Potential $\phi(\mathbf{x})$

The density of the ions is not affected by the potential. Therefore, the structure of the ion density is given by simple cones which describe the thermal diffusion of the ions into the wake. The densities of the plasma- and photo-electrons, however, are strongly influenced by interaction with the potential $\phi(\mathbf{x})$.

2.1. A Two-Dimensional Model for Numerical Plasma Simulation

The motion of the solar wind around the probe and the development of the potential $\phi(\mathbf{x})$ is calculated by means of a two-dimensional model with simplified probe geometry. This is not able to describe the real three-dimensional situation correctly, but it may be used as a tool to understand the essential interaction between plasma and spacecraft. Moreover, the two-dimensional model is chosen in order to save computer time and storage requirements.

The floating potential of the probe is calculated from the balance of currents arriving at the probe or leaving it. With increasing simulation time, the floating potential reaches a stationary value with only small statistical fluctuations.

The plasma electrons are simulated as discrete (super-) particles by the particle-in-cell method (Morse, 1970; Birdsall et al., 1970). They are created at the outer boundaries of the simulation region according to the undisturbed distribution function. A Maxwellian distribution, shifted according to the solar wind bulk velocity, it assumed for that purpose. Several thousand particles are moved together in the potential like real electrons and the potential is updated from the resulting charge density at every time step. The path of any particle is followed until it leaves the simulation region or until it reaches the surface of the probe and contributes to the current balance. Photoelectrons with a mean energy of only 1 eV are emitted from the sunlit side of the probe. They are regarded as a third constituent of the plasma. For their number density an approximation is used (Schröder, 1974) which describes the strong interaction with the potential $\phi(\mathbf{x})$. Another approximation gives the amount of negative charge transported from the surface into the undisturbed plasma region (Könemann, Schröder, 1974) as dependent on the surface potential.

For further details concerned with this model, the reader may be referred to Isensee (1975).

2.2. Results

In order to obtain the potential $\phi(\mathbf{x})$, the simulation program was executed with a simulation area of $9\,\mathrm{m} \times 19.75\,\mathrm{m}$, divided into $0.25\,\mathrm{m} \times 0.25\,\mathrm{m}$ cells. Up to 10^4 particles have been used, each representing $1.5 \cdot 10^6$ electrons. With a time step of $7.5 \cdot 10^{-8}\,\mathrm{s}$, the potential reached a stationary value yielding the self-consistent potential in the Vlasov-Poisson system after approx. 200 steps. The simulation process has been continued for about 300 additional steps to average out the statistical fluctuations which are due to the mathematical method. Then the

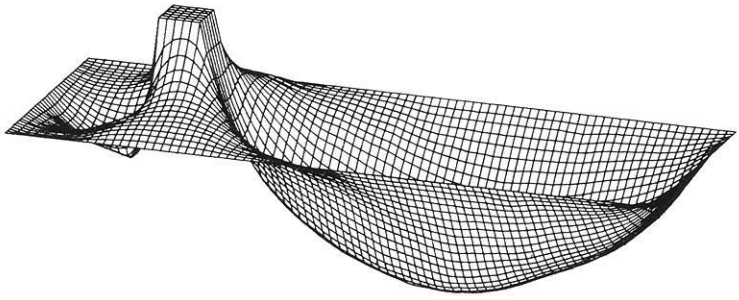

Fig. 1. The potential $\phi(\mathbf{x})$ for solar wind conditions at 0.2 AU distance from the sun. The solar wind flows from the left to the right. The spacecraft is represented by the square with a surface potential of 2.9 V. The minimum in front of the probe (-1.4 V) is due to the photo electron cloud. The minimum in the wake has a depth of -4.5 V

potential $\phi(\mathbf{x})$ is used as input data for subsequent calculations. This model for the potential is shown in Figure 1. The floating potential of the probe surface has the value of 2.9 V. The potential is characterized by the negative minima. Behind the probe is a region of very low ion density. This results in an expanded region of negative potential with a minimum of -4.5 V. A very dense cloud of photoelectrons develops immediately in front of the sunlit side of the probe. This is the reason for the second negative minimum with -1.4 V.

At greater distances from the sun, the negative minima are less distinctive. At 1.0 AU distance, the very rarefied plasma modifies the vacuum potential ($\Delta\phi = 0$) only slightly. With increasing distance from the sun, all particle densities decrease in the same way (inverse square law). This effect would keep the floating potential constant. However, the floating potential depends on the current densities; therefore it also depends on the temperatures. The temperature of the photoelectrons is constant. The plasma electron temperature, on the other hand, decreases, resulting in a smaller plasma electron current. The result is that the floating potential assumes a higher value with increasing distance from the sun.

3. Distortion of Distribution Function

In this chapter, let us assume that a measuring instrument is located at the surface of the spacecraft. It is considered as a device that counts electrons coming from a discrete direction but with different energies to give a velocity distribution function $f_s(\mathbf{v})$ at the location $\mathbf{x}_s$ on the surface of the probe.

The instrument detects the electrons that have penetrated the potential in the vicinity of the probe, but cannot detect those undisturbed electrons far away from the probe directly. Therefore the velocity distribution measured by the instrument differs from the undistorted distribution present in the solar wind.

Because of the positive surface potential, all electrons have been accelerated. That means that no plasma electrons can be counted below an energy that corresponds to the surface potential. This energy range is filled by photoelectrons emitted from the surface.

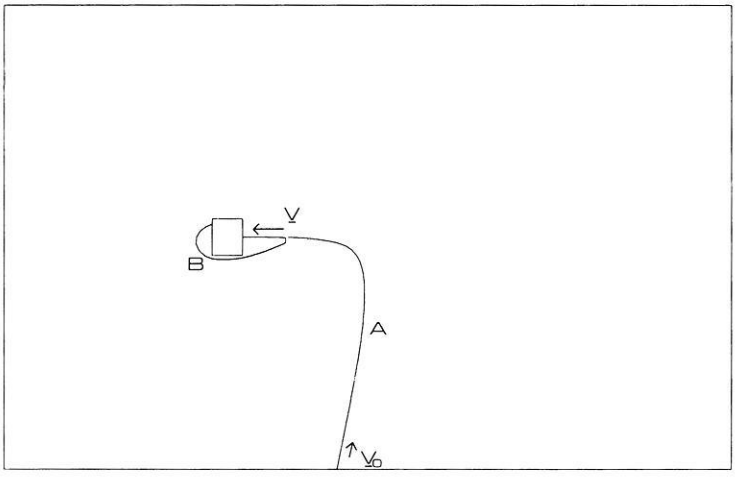

Fig. 2. The method of retracing electron trajectories. Electrons with the initial velocity $\mathbf{v}_0$ in the undisturbed solar wind are deflected by the potential and arrive at the probe with the velocity $\mathbf{v}$ (case a). Photoelectrons are deleted from the distribution f_s (case b)

3.1. The Method: Characteristics of the Vlasov Equation

The velocity distribution function $f(\mathbf{x}, \mathbf{v})$ for the plasma electrons is the solution of the Vlasov equation

$$\mathbf{v} \cdot \nabla_x f(\mathbf{x}, \mathbf{v}) + e/m \nabla_x \phi(\mathbf{x}) \cdot \nabla_v f(\mathbf{x}, \mathbf{v}) = 0 \tag{1}$$

with the potential $\phi(\mathbf{x})$ from chapter 2.

The equation is solved for $f(\mathbf{x}, \mathbf{v})$ by means of the fact, that the distribution function f is a constant along a path in phase space, i.e. the trajectories in phase space are the characteristics of the partial differential equation (1) (Courant, Hilbert, 1968). If the points $(\mathbf{x}_1, \mathbf{v}_1)$ and $(\mathbf{x}_2, \mathbf{v}_2)$ in phase space are connected by a trajectory, then

$$f(\mathbf{x}_1, \mathbf{v}_1) = f(\mathbf{x}_2, \mathbf{v}_2). \tag{2}$$

In order to calculate the distorted value $f_s(\mathbf{v}) = f(\mathbf{x}_s, \mathbf{v})$ at a certain point $\mathbf{x}_s$ on the surface of the probe, the path of an electron arriving at that point with the velocity $\mathbf{v}$ is followed back through the potential (Fig. 2). Two cases are possible:

(a) If the electron has come from the undisturbed solar wind region with the initial velocity $\mathbf{v}_0(\mathbf{x}_s, \mathbf{v})$, then

$$f(\mathbf{x}_s, \mathbf{v}) = f(\mathbf{x}_0(\mathbf{x}_s, \mathbf{v}), \mathbf{v}_0(\mathbf{x}_s, \mathbf{v})) \tag{3}$$

or

$$f_s(\mathbf{v}) = f_M(\mathbf{v}_0(\mathbf{x}_s, \mathbf{v})) = \exp(-m/2kT(\mathbf{v}_0 - \mathbf{w}_0)^2). \tag{4}$$

f_M is the undisturbed Maxwellian distribution in the solar wind with the bulk velocity $\mathbf{w}_0$. It is independent of the position $\mathbf{x}_0$.

(b) If the electron has come from the probe surface, then

$$f_s(\mathbf{v}) = 0. \tag{5}$$

That means that photoelectrons emitted from the surface are not taken into account in calculating the distribution.

It is important that the electric fields modify the absolute values of the velocities as well as the direction of the incoming electrons. The difference between the absolute values of $\mathbf{v}$ and $\mathbf{v}_0$ is easily derived from the energy conservation.

$$\mathbf{v}_0^2 = \mathbf{v}^2 - 2e/m\phi_s \tag{6}$$

with the surface potential ϕ_s.

The result of these changes of the absolute values of the velocities alone would be a simple shift to higher energies. The following figures show this kind of curves as reference spectra $f_r(\mathbf{v})$.

$$f_r(\mathbf{v}) = \begin{cases} f_M(|\mathbf{v}_0|\,\mathbf{v}/|\mathbf{v}|) & \text{if } \mathbf{v}^2 - 2e/m\phi_s \geqq 0 \\ 0 & \text{if } \mathbf{v}^2 - 2e/m\phi_s < 0 \end{cases} \tag{7}$$

The differences between f_s and f_r are the result of the deviation in the direction of the inital velocity $\mathbf{v}_0$ together with the anisotropy of the streaming solar wind plasma. The trajectories become more probable with an initial velocity more parallel with the bulk velocity $\mathbf{w}_0$. That gives a greater value of f_s. To emphasize the effects of the curvature of the electron trajectories, the curves are calculated with a high solar wind velocity ($w_0 = 800$ km/s).

3.2. Results

The negative charge densities by volume result in regions of negative potential. This leads to the following disturbances of the electron velocity distribution at the surface of the probe:

(a) Plasma electrons with very low energy may be reflected by the potential minima. This results in an energy range above the surface potential in which no plasma electron can be counted by the instrument.

(b) The trajectories of electrons with a little more energy are curved considerably. This results in modifications of the distribution together with the anisotropy of the solar wind plasma (which is due to the bulk velocity $\mathbf{w}_0$). Generally speaking, in this energy range the number of electrons decreases at the front of the probe and increases at the rear.

Electrons with energies above 20 eV are hardly influenced by the potential.

These main effects of the negative potential minima are shown in the following two examples.

The spectra in Figure 3 simulate a measurement in antisolar direction. At energies above 20 eV there is no difference between the distribution function and the reference curve. With decreasing energy, the number of electrons arriving from antisolar direction becomes greater than indicated by the reference curve. The reason is the deflection by the negative wake as shown in Figure 4. The initial value of the velocity in the undisturbed solar wind becomes more and

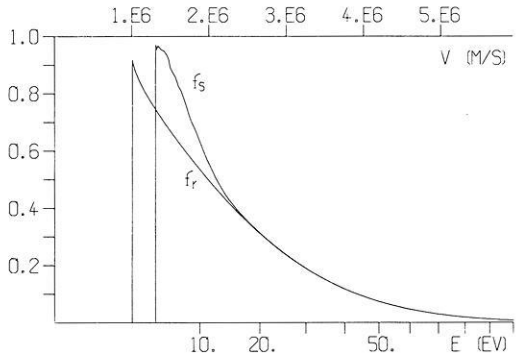

Fig. 3. Disturbed distribution function f_s and reference curve f_r for a measurement in antisolar direction (cf. Fig. 4)

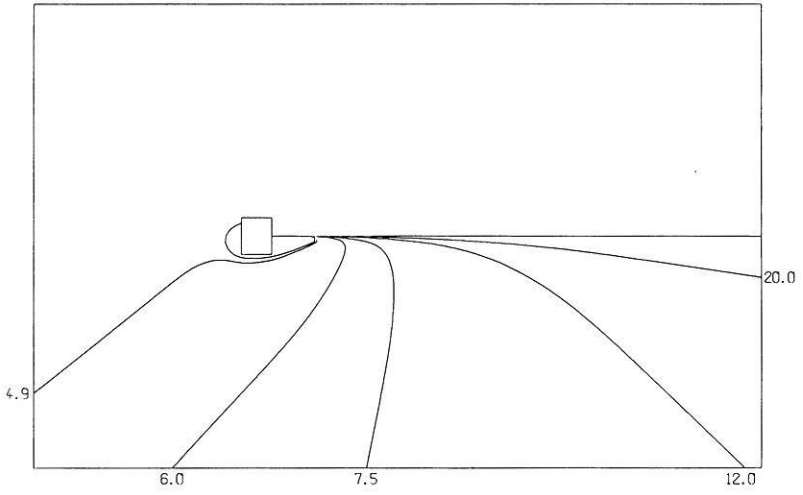

Fig. 4. Examples of trajectories of electrons arriving at the probe from antisolar direction. The numbers denote the energy in eV belonging to the trajectory. The deflection of the electrons by the wake is demonstrated

more parallel with the bulk velocity – the number of electrons increases (see Eqs. (4) and (7)). Below 4.9 eV, no electrons can be detected from antisolar direction: they are screened by the wake. In addition, Figure 4 shows a possible path for photo electrons reaching the measuring instrument at the back side of the spacecraft, in spite of an energy (4.8 eV) above the surface potential (2.9 eV). Figures 5 and 6 show the influence of the photo electron cloud. The instrument is situated at the front of the probe. The angle of incidence of the electrons is 30 degrees. Electrons counted between 5 eV and 10 eV are reflected at the potential minimum in front of the probe, their initial velocities have been nearly perpendicular to the bulk velocity. In the range between 4 eV and 5 eV the direction of the initial velocity is again more parallel to the bulk velocity, since the electrons are reflected at the wake before they come under the influence of the photoelectron minimum. This results in the peak within the distribution function.

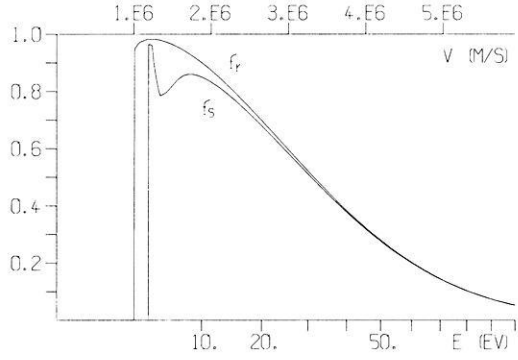

Fig. 5. Distribution for a measurement at the front side with an angle of incidence of 30 degrees (cf. Fig. 6)

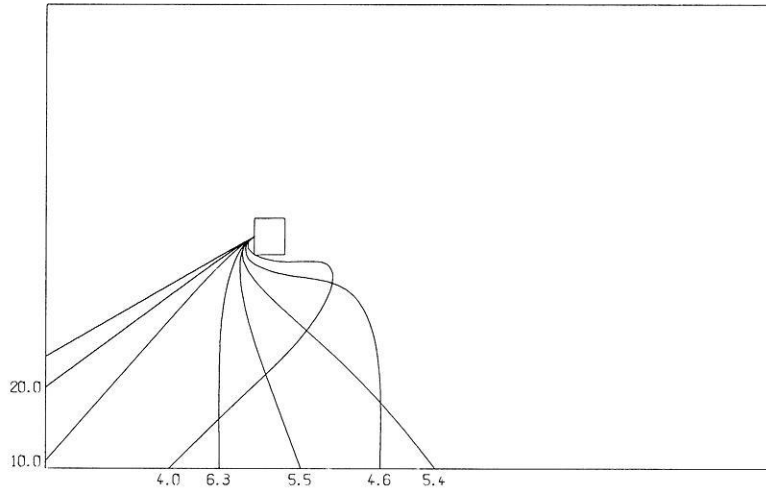

Fig. 6. Examples of electron trajectories concerning Figure 5. In the energy range between 4 eV and 5 eV the electrons are first deflected at the wake before being directed into the instrument by the photoelectron minimum

4. Conclusions

The two-dimensional model enables us to calculate modifications of the electron velocity distribution which are caused by the charge densities in the wake and by the photo electron cloud. These disturbances must be taken into account for a correct interpretation of the electron distribution measurements in the low energy range. However, it must be emphasized that the effects of non-conductive probe surface elements (solar cells) are of the same order of importance as the disturbances described in this paper. The effects of non-conductive probe surfaces are not included in the present model as yet but must be considered in future work.

Acknowledgement. This work was partially supported by a grant of DFVLR-BPT Nr. 01QCO26A-Z24WRSO108 (project HELIOS). I am indepted to Dr. G.H. Voigt and H. Massberg (TH Darmstadt, Angewandte Geophysik) for many fruitful discussions.

Major parts of this paper were completed at the Technische Universität Braunschweig, Lehrstuhl B für Theoretische Physik under the direction of Prof. Richter. I am greatly indepted for his kind support.

References

Birdsall, Ch.K., Langdon, A.B., Okuda, H.: Finite-Size Particle Physics Applied to Plasma Simulation: in Methods of Computational Physics, **9**, New York and London: Academic Press 1970

Courant, R., Hilbert, D.: Methoden der mathematischen Physik, 2nd ed. Berlin-Heidelberg-New York: Springer 1968

Isensee, U.: Anwendung numerischer Plasmasimulation bei der Berechnung von Plasmastörungen durch ein Raumfahrzeug im solaren Wind. BMFT-Forschungsbericht FBW 75-20, 1975

Könemann, B., Schröder, H.: Planet. Space Sci. **22**, 321–331, 1974

Morse, R.L.: Multidimensional Plasma Simulation by the Particle-in-Cell Method: in Methods of Computational Physics, **9**, New York and London: Academic Press 1970

Schröder, H.: Thesis, Lehrstuhl B für Theoretische Physik, TU Braunschweig, 1974

Received November 29, 1976; Revised Version May 20, 1977